Available online at www.sciencedirect.com

SCIENCE DIRECT®

Tectonophysics xx (2004) xxx–xxx

TECTONOPHYSICS

www.elsevier.com/locate/tecto

Geodynamics of continental plate collision during late tertiary foreland basin evolution in the Timor Sea: constraints from foreland sequences, elastic flexure and normal faulting

John Londono*, Juan M. Lorenzo

Department of Geology and Geophysics, Louisiana State University, E235 Howe-Russell Complex, Baton Rouge, LA 70803, USA

Abstract

Tectonic subsidence of the Australian lithosphere during the Late Tertiary propagates from the southwest to the northeast in the Timor Sea, as a consequence of the oblique collision between the Eurasian and Australian plates. We reconstruct the asynchronous nature of deflection of the Australian plate created during the plate convergence by best-matching the geometry of de-compacted foreland strata against the predictions of simple bending elastic beam models. We infer a maximum subsidence of 3500 m and a maximum width for the basin of ∼470 km. The effective elastic thickness of the Australian lithosphere (∼80 to 100 km) does not change significantly during basin evolution. The low curvature imposed on the plate ($\sim 5.1 \times 10^{-8}$ m^{-1}) during bending is too small to weaken the plate. Yet, abundant but small-slip, normal faulting related to bending implies some degree of inelastic yielding. The polarity of fault propagation supports the oblique nature of the collision. Flexural models indicate that at least 570 km of Australian plate (mostly areas of stretched continental crust) was flexed, primarily by the tectonic loading of the Timor Island and that the total amount of subducted plate was at least 100 km during basin evolution.

Keywords: Geodynamics; Lithospheric flexure; Timor Sea; Eurasia–Australia collision

1. Introduction

Foreland basin subsidence is primarily related to the vertical deflection of the lithosphere caused by loading of orogenic belts, although subsurface loads, and sediment and water bodies also play an important role in the process. The distinctive wedge-like geometry of foreland basins is a direct result of asymmetric subsidence caused by the accumulation of vertical stresses toward the deeper end of the plate. The stratigraphic record complies with the regional architecture and therefore represents the geometry of the basin at depositional time (Beamont, 1981; Dorobek, 1995; Kruse and Royden, 1994; Turcotte and Schubert, 1982; Yang and Dorobek, 1995). The timing, amount of vertical force and total plate deflection may be determined via flexural modeling, using the stratigraphic record deposited during tectonic loading. The basin-subsidence can be modeled as the flexural response of an elastic plate to a vertical linear load (Turcotte and Schubert, 1982). Changes in subsidence

* Corresponding author. Tel.: +1-225-578-2680; fax: +1-225-578-2302.

E-mail address: jlondono@geol.lsu.edu (J. Londono).

0040-1951/$ - see front matter © 2004 Published by Elsevier B.V.
doi:10.1016/j.tecto.2004.04.007

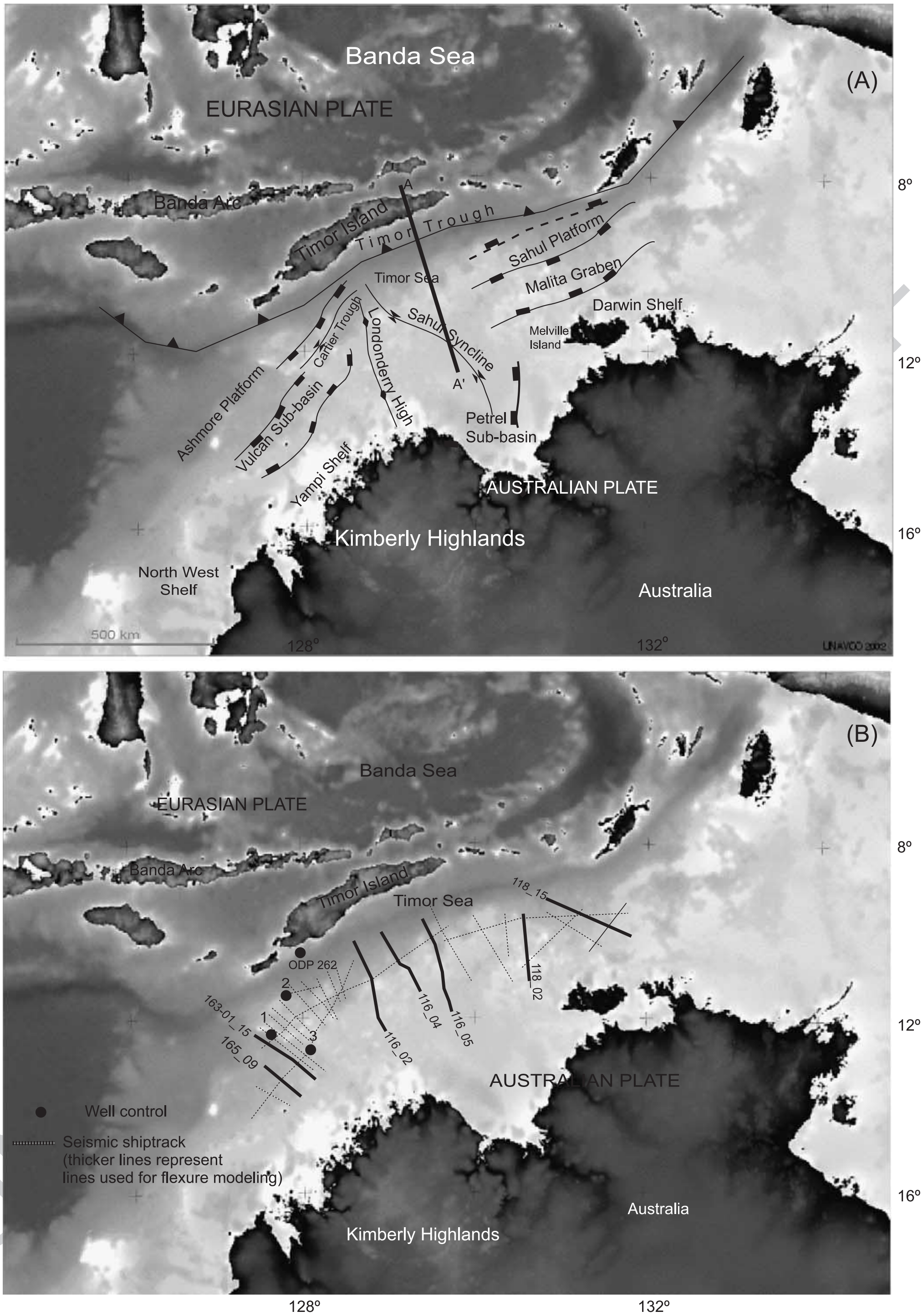

Fig. 1. (A) Tectonic setting of the Timor Sea. A–A′ cross-section in Fig. 2. (B) Seismic and well data. Line number as referred by AGSO. Wells: (1) Ashmore Reef 1; (2) Delambre 1; (3) Buffon 1.

across the strike of the basin through time document the amount (Cardozo and Jordan, 2001) and polarity of loading, and the variation in lithospheric strength. Normal faulting has been reported along the subducting plates as an effect of the flexing lithosphere undergoing inelastic deformation (e.g. Bradley and Kidd, 1991). Extensional faulting is expected to affect areas of high curvature within the upper half of the bending plate. Variations in the amount of tectonic transport of the overridden plate trough time change the amount of bending and the spatial distribution of associated normal faults. The forebulge, a lithospheric protuberance developed as an elastic effect of the deflection on the landward end of the bending plate, is expected to reach highs of up to hundreds of meters and to extent over hundreds of km. It is usually recognized by unconformities and sedimentary pinch-outs on both of its flanks.

The Late Tertiary foreland basin that developed in the Timor Sea (Fig. 1) during the latest episode of collision between the Australian and Eurasian plates (~6.5 to 1.6 Ma) provides an excellent example of a peripheral foreland basin (Lorenzo et al., 1998; Miall, 1995; Tandon et al., 2000). The Timor Trough, a deep depression, is created by the deflection of the Australian plate under the load of the accretionary wedge (Hamilton, 1979; Harris, 1991), as well as sediment and sub-surface loading (Lorenzo et al., 1998). Tandon et al. (2000) and Lorenzo et al. (1998) used sea floor bathymetry and gravity data to determine the present lithospheric strength of the Timor Sea foreland basin. They modeled the present geometry of the Timor Trough as a ~300 km wide, ~2000 m deep depression with a 300 m high forebulge (Fig. 2). The Australian continental shelf has been heavily affected by reactivation and/or new growth of normal faulting during foreland evolution. Lorenzo et al. (1998) emphasize the role of normal faulting as evidence of inelastic yielding during bending of the Australian plate. O'Brian et al. (1999) recognize the role of plate down-warping in the reactivation of Jurassic faults and formation of Mio-Pliocene fault arrays. Some of these faults are still active, as shown by vertical displacement of the present sea floor (Lorenzo et al., 1998).

This manuscript is relevant to the present special issue of *Tectonophysics* because it deals with the continental margin evolution of the Pacific Rim, in particular the geodynamics of a well-documented collision zone in the Australia–Indonesia region,

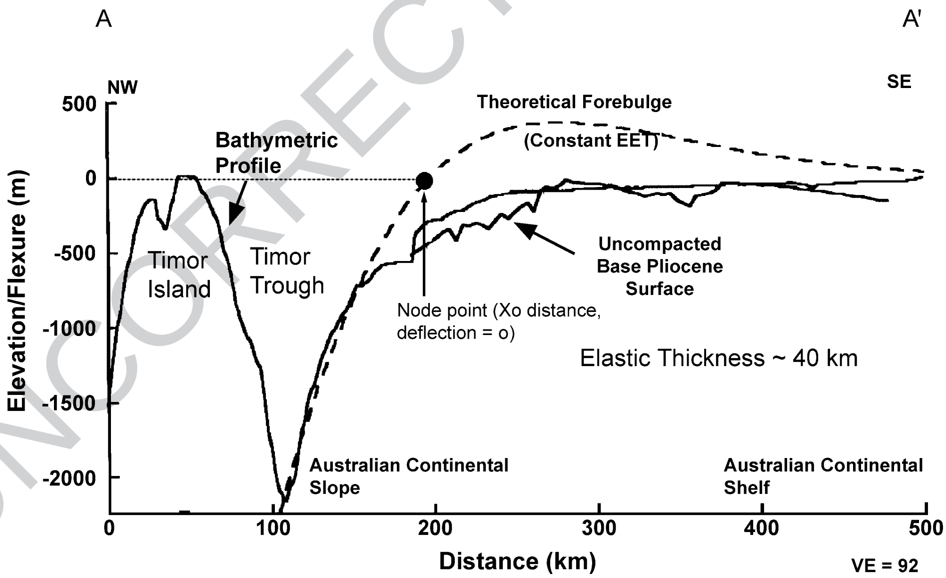

Fig. 2. Present Timor Sea/Timor Trough flexural model, modified from Lorenzo et al. (1998). Extent of effective plate from node point (point of zero deflection and marks the beginning of the forebulge) is ~230 km for continuous model and ~155 km for broken plate. The flexural parameter (α) is ~98 km (see Fig. 1A for location).

along the Timor Sea foreland basin. This unique, early-stage foreland basin has not been disrupted by later tectonics. Therefore it can be used to study how the Australian plate has reacted to vertical loading trough time. We use flexural models representing the bending plate to estimate the effective elastic thickness during evolution of the basin. We calculate the amount of loading, infer the nature of the collision between the Eurasian and Australian plates and characterize how the Australian lithosphere has responded to the load of the Banda Orogen accretionary prism. The position of the geodynamic elements of the bending plate model during basin evolution provides a tool to reconstruct the regional basin history in terms of subsidence (deflection), tectonic transport (linear load position) and the extent of the Australian lithosphere flexed by loading. We also evaluate the impact of inelastic yielding and of the curvature caused by vertical loading on plate strength. The timing of the apparent displacement of new or reactivated faults developed during the evolution of the foreland basin is used as an indicator of the polarity of collision. Our results, based mainly on extensive seismic data, indicate that despite continuous deformation through time, no significant change in lithospheric strength has occurred during foreland development. We also recognize the NNE oblique nature of plate collision in the Timor Sea. The amount of deflection and inelastic deformation in the southwestern part of the Timor Sea reveals that this area has undergone deformation and has been heavily affected by tectonic loading since Late Miocene time. In contrast, in the northeastern region the effect of loading has been more substantial since Late Pliocene time.

2. Tectonic setting

The northwestern Australian continental plate is presently at a steady-state collision with the Banda arc and Timor Island (Hamilton, 1979; Fig. 1). The colliding process began to affect the Australian North West Shelf in the Timor Sea in Late Miocene times. The N20E convergence of the Australian plate is estimated at a rate of 71 mm/year (Tregoning et al., 1994). However, GPS studies (Genrich et al., 1995) indicate that the Australia–Timor convergence has ceased and the Australia–Eurasia collision is accommodated by back-thrusting north of Timor along the Flores and Wetar thrusts. The Australian lithosphere has been subducted under a 200 km wide zone of Eurasian lithosphere (Richardson and Blundell, 1996), including Timor Island, an accretionary prism (Audley-Charles, 1986) developed over part of the stretched Australian continental crust. The Australian North West Shelf in the Timor Sea has experienced various tectonic episodes since Paleozoic times. O’Brien et al. (1996) note that NE–SW trending structures (Vulcan and Malita grabens, Fig. 1) reveal Late Devonian–Early Carboniferous rifting events, in contrast to the NW–SE trend of Jurassic rift-related basins (Pretelt sub basin, Sahul Syncline, Fig. 1). Hamilton (1979), using refraction velocities, reports more than 4 km of sedimentary cover overlying continental crust at the toe of the tectonic wedge. Continental crust with decreasing thickness, from 35 km in Kimberly Highs to 26 km under the outer shelf near the Timor Trough (Petkovic et al., 2000), underlies the Australian shelf. Petkovic et al. (2000) estimate the attenuation of Precambrian basement rocks from 35 to 13–14 km across the margin ($\beta = 2.6$).

2.1. Foreland stratigraphy

Since the Late Miocene, the North West Australian Shelf in the Timor Sea has been a carbonate ramp whose stratigraphic architecture has been driven principally by sea level fluctuations of diverse origin, such as tectonic subsidence and eustasy (Apthorpe, 1988). Two unconformities have been identified in the foreland succession (Fig. 3). The oldest one, at the base, interpreted from the juxtaposition of shallow and deepwater facies, was identified in the commercial wells Delambre 1 and Buffon 1 (Fig. 1; Apthorpe, 1988). This regional unconformity, at the top of Middle Miocene limestones (planktonic forams of Zone N10), is overlain by Late Miocene carbonate sediments of deep water nature (Zone N15). The second unconformity, reported by Veevers (1974) at the ODP Leg 262, separates shallow water upper Pliocene dolostones and calcarenites from folded shallow-water lower Pliocene carbonates, at the axis of the trough. Boheme (1996) also identifies this unconformity along proprietary seismic profiles. According to Hillis (1992), the hiatus represents a short-term depositional break (< 1 Ma) at Ashmore

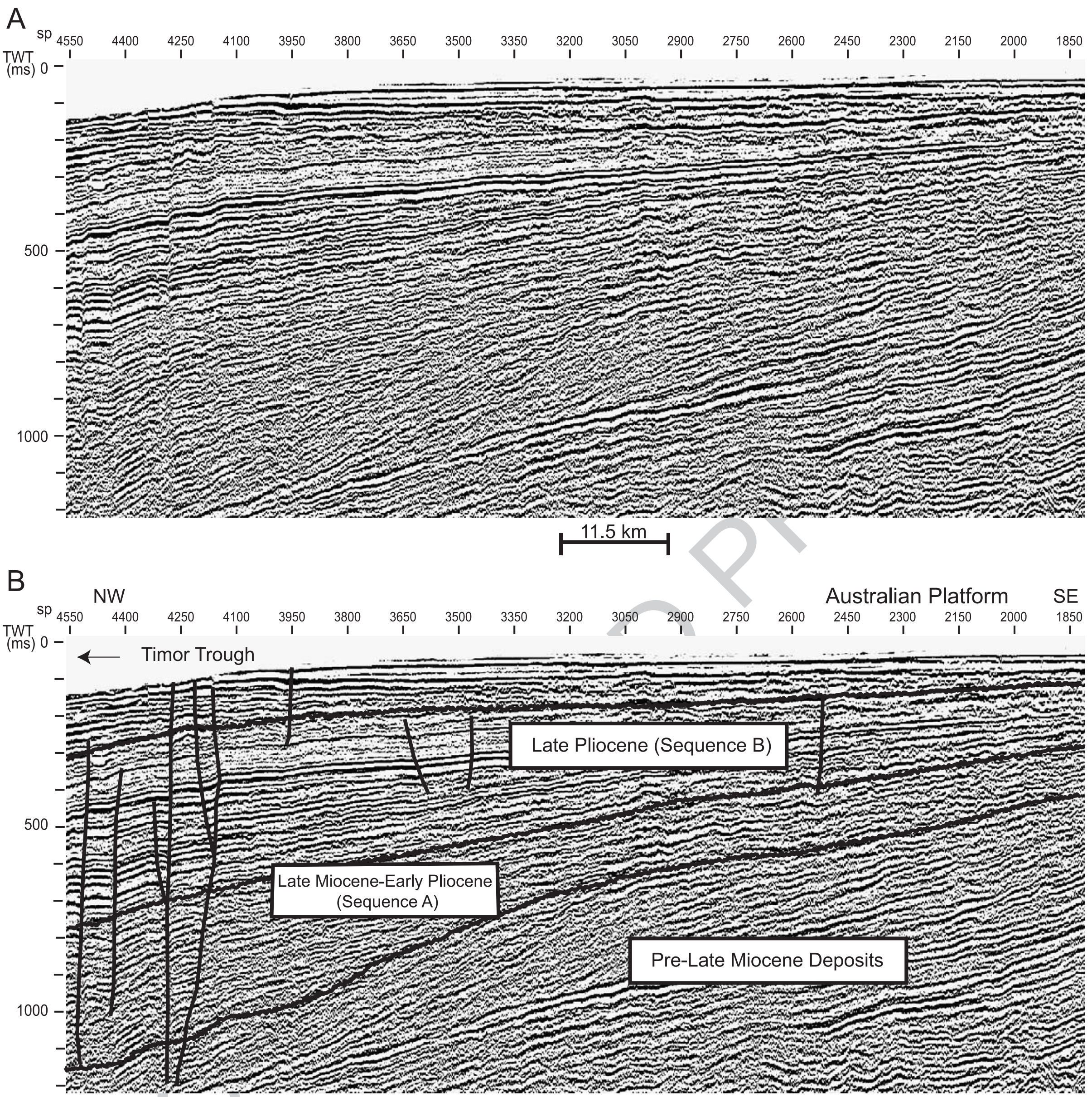

Fig. 3. (A) Uninterpreted Seismic Line 118_15 (see Fig. 1 for location). (B) Interpreted seismic profile. Well data and previous interpretations were used as constrains. Note the characteristic regional wedge-like geometry of the foreland succession (highlighted by black lines). Interval-velocity range is between 1500 and 2200 m/s. The boundaries of the sequences are short-term unconformities. New faults were developed during plate bending and older normal faults were reactivated.

Reef 1 well (Fig. 1). The top of the foreland deposits are punctuated by the youngest lithified sediments dated at ~1.6 Ma (Apthorpe, 1988). The lithology of the entire succession, poorly known, is described in some wells as greenish-gray calcilutites and calcisiltites (sic.) of outer shelf, shelf edge and platform environments (Apthorpe, 1988).

The seismic reflectors that represent the top of Late Pliocene and the unconformities at the base of Late Miocene and Late Pliocene are identified within our seismic data. The interpretation (Fig. 3) was carried out by integration of well information (sequence thickness and age) and previous reports (Ostby and Johnstone, 1994; Woods, 1994; Wormald, 1988) based on seismic data (reflector geometry, interval time and thickness). Since our goal is to analyze the temporal evolution of the foreland basin, we divide the foredeep succession in two packages, as does Boheme (1996). Using the regional unconformities we named the oldest Sequence A (Late Miocene to Early Pliocene) and the youngest Sequence B (Late Pliocene). The present combined thickness of these sequences varies between 20 and 800 m.

3. Data

Over 2000 km of two-dimensional seismic reflection data, 4 to 6 s recording, 48-fold coverage, from 192 channels with 50 m shot interval and 12.5 m common-depth points (CDP's) from the Australian Geological Survey Organization (AGSO) 1996 seismic program (Fig. 1) are used as the primary source of data. Most shiptrack lines are parallel to the SSE Miocene-to-Recent tectonic transport direction. Although seismic profiles only sample the Australian shelf and southern Timor Trough, they contain enough information for flexural modeling. Additionally, well log information and seismic data from the literature allow us to tie biostratigraphic and lithological data to the seismic record (Figs. 1 and 3).

4. Methods

Sequence boundary unconformities are mapped within the entire seismic data. Areas like the Cartier Through, where the interpretation is ambiguous due to high deformation, are omitted from subsequent flexural analysis. The largest uncertainty in the reconstruction of de-compacted thickness and flexure profiles is associated with estimates of sequence thickness calculated using interval velocities derived from the seismic semblance analysis. According to our seismic data, interval velocities between 1500 and 2500 m/s appear to be the most suitable for the foreland deposits. These velocities agree with previous interpretations of proprietary data in the area. For this two-end member interval velocity range, the error in thickness calculation might be 11% to 14%. The results, where control is possible, match the thickness range constraint by well information. Isopach maps derived from our seismic interpretation (Fig. 4) show local depocenter distribution within the general deepening of the basin during foredeep sedimentation.

4.1. Flexural models

We assume that the accommodation space in the evolving Timor Sea foreland basin is completely filled with sediments throughout the two depositional periods we are analyzing. Unfortunately, there is not enough data to constrain the water depth at any time. Thus, we take the base of the sequence profile, at a particular period, to represent the down-warping top of the lithosphere and the top of the profile as a horizontal surface. This, ideally flat surface, rarely coincides with sea level; rather, it is an abstraction that represents a horizontal datum of zero deflection and marks the position of node point along the profile, as well as the beginning of the forebulge (Fig. 2). These profiles are used as the principal constraint to develop models of plate deflection. The theoretical curves, produced primarily by variation in effective elastic thickness and in amount of loading, must match adequately the geometry of the data (de-compacted thickness profiles) and fit into the geological model of the basin. We reproduce the theoretical profiles following the mechanical model of the two-dimensional flexure of an elastic beam, of constant elastic thickness, lying over a viscous substratum (Turcotte and Schubert, 1982). Table 1 summarizes the parameters used in these calculations. Seven seismic profiles were chosen to carry out flexural modeling (Fig. 1). We discard lines crossing areas deformed by salt-tectonics and consider only seismic lines collected parallel to the regional NW–SE tectonic load transport direction.

Foreland basin studies use both broken and continuous plate models. For example, Tandon et al. (2000) use a broken plate for modeling the Australian Shelf, whereas Kruse and Royden (1994) use a continuous plate model for the Apennine and Dinaride foreland basins in the Adriatic Sea. Using the present bathymetric profile of the oceanic floor in the Timor Sea (Fig. 2), we test both continuous and broken plate models. In the first case, the point of maximum

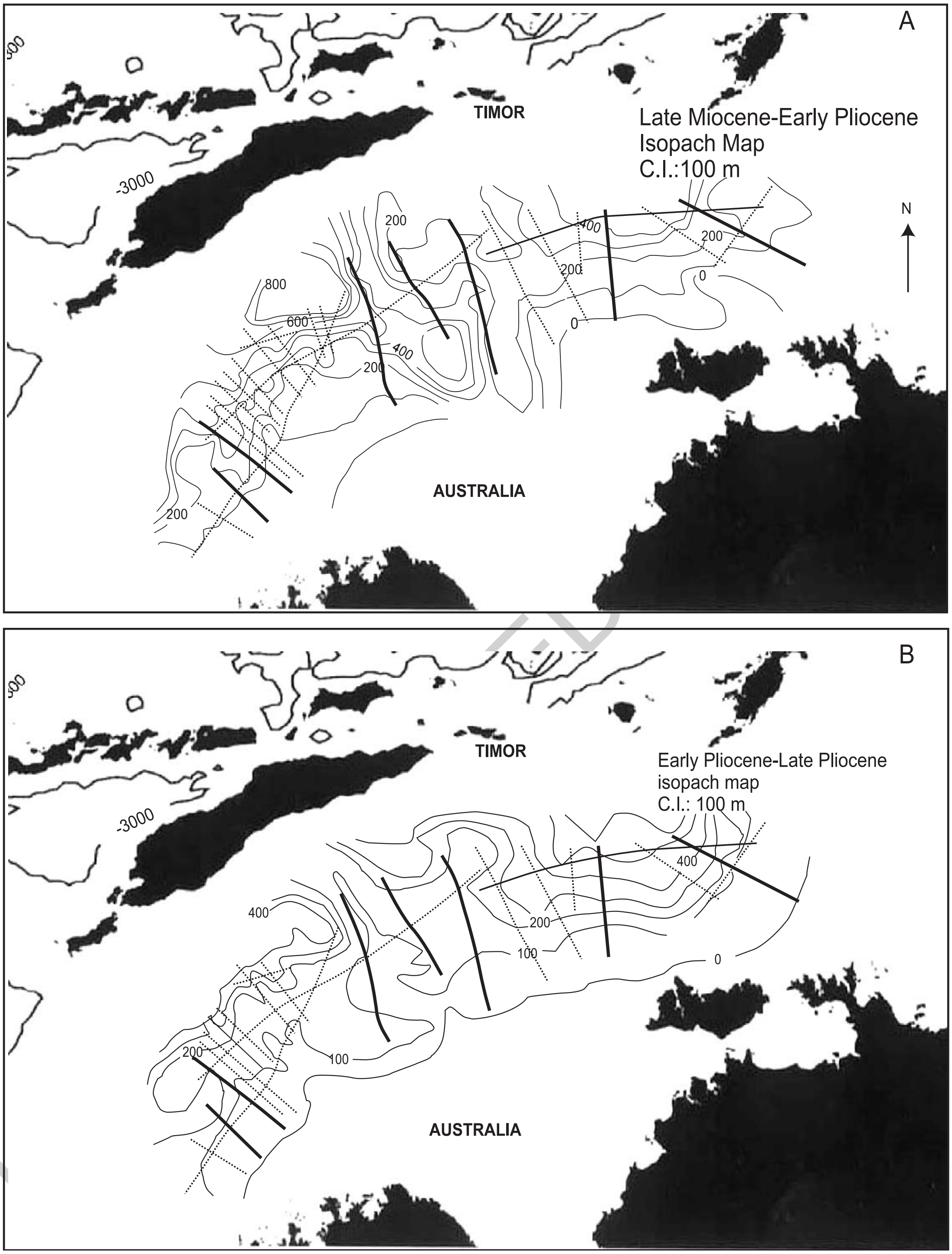

Fig. 4. Isopach maps for Late Miocene–Early Pliocene (A) and Early Pliocene–Late Pliocene (B). Note the increasing thickness toward the trench. Map A shows some regional tectonic structures like the Sahul Syncline and Vulcan Sub-basin. In Sequence B (map B) no structure is clearly distinguishable from the isopach map.

Table 1
Geodynamic constants

Definition	Symbol	Value/units
Density of water	ρ_w	1030 kg/m^3
Density of mantle	ρ_m	3300 kg/m^3
Flexural rigidity	D	Nm
Effective elastic thickness	Te	km
Flexural parameter	α	m
Maximum deflection	W_o	m (at point Xo)
Gravitational acceleration	g	9.8 m/s^2
Young modulus	E	11×10^{11} Pa
V	Poisson Ratio	0.25
Load (linear)	P_o	N/m
Bending moment	M	N
Curvature	R	1/m

Summary of the mechanical parameters used in the models. The governing equation for the bending plate is $D(d^4w/dx^4)+(\rho_m-\rho_w)gw=0$ (Turcotte and Schubert, 1982) assuming a linear load, where D is flexural rigidity, w is the deflection, ρ_m is the density of the mantle, ρ_w the density of water infill, g gravity acceleration. Bending moment (M) is given by equation $M=D(d^2w/dx^2)$. Curvature is given by equation $R=M/D$ (Turcotte and Schubert, 1982).

deflection is located 231 km from the node point, ~100 km north of the western margin of Timor Island. For a broken plate model the maximum extent of the effective plate is 154 km, and the end of the plate is located directly below Timor Island. Both models match the data using an effective elastic thickness of ~40 km. However, we consider that the assumption of a continuous plate gives more reliable results. This assumption is based on tectonic models (Karig et al., 1987) and seismic studies (Hamilton, 1979; Veevers, 1974) showing the Australian plate going beyond the present position of the Banda Arc.

It is important to consider the position of our data within our modeled profiles at each particular time (Figs. 1 and 2). Our study area undergoes NNW displacement with respect to the Eurasian plate during collision. The same well location, for example, will over time occupy a point closer to the trench. Consequently, within each profile the seismic data partially records at least two independent flexed stages of the plate. Sequence A contains sediments deposited more distally from the trench axis, while Sequence B contains sediments deposited at sites more proximal to the trench axis. Today's position of the seismic data is assumed to be at the most proximal position to Timor Island (tectonic load). Therefore the present distances between the point of zero deflection (node point, Fig. 2) and the position of the linear load (Point of maximum deflection Xo, Table 1, Figs. 5 and 6) must be the minimum acceptable value for our models.

4.2. De-compaction calculation

Sediment de-compaction is carried out to obtain the thickness at the time of deposition. For this calculation we assume a porosity–depth function $\phi=\phi_0 e^{-cz}$ (Allen and Allen, 1990; Lerche, 1990), where ϕ is the estimated present-day porosity and z the present depth below sea level. Values for c, the ϕ-depth curve-slope coefficient (0.57 km^{-1}); and ϕ_0, initial porosity (0.63), are taken from studies based on well-logs in the Australian platform (Hillis, 1990).

Sediments are de-compacted following Steckler and Watts (1980), using the function $S=h(1-\phi)/(1-\phi_0)$, where S is the thickness of the de-compacted layer (sequence) and h the present-day thickness. We assume that compaction is the product of decreasing porosity due only to the mechanical non-reversible process of expulsion of pore water.

From the thickness error introduced by interval velocities inaccuracy, porosity can change up to ~3%. This in turn introduces an error in de-compacted thickness up to ~7%, which we consider an acceptable value since the average thickness change is ~28%.

4.3. Flexure-related normal faulting

Reactivated normal fault planes dip between 33° and 40° in the shallow section within post Cretaceous sediments. In the deeper section, some faults are listric and their traces die out in pre-Mesozoic strata, irrespective of fault vergence (Fig. 3). A regional detachment zone is not easily distinguishable along the seismic data; nonetheless, Paleozoic evaporite beds are the most probable detachment level in the area. O'Brien et al. (1993) report some of these faults cutting basement at 15 to 20 km depths. Newer faults, developed during foreland evolution, die within Cretaceous or younger strata and dip between 40° and 55° along the entire fault trace.

We assume that the fault slip measured along the fault plane in the foreland basin deposits indicates a

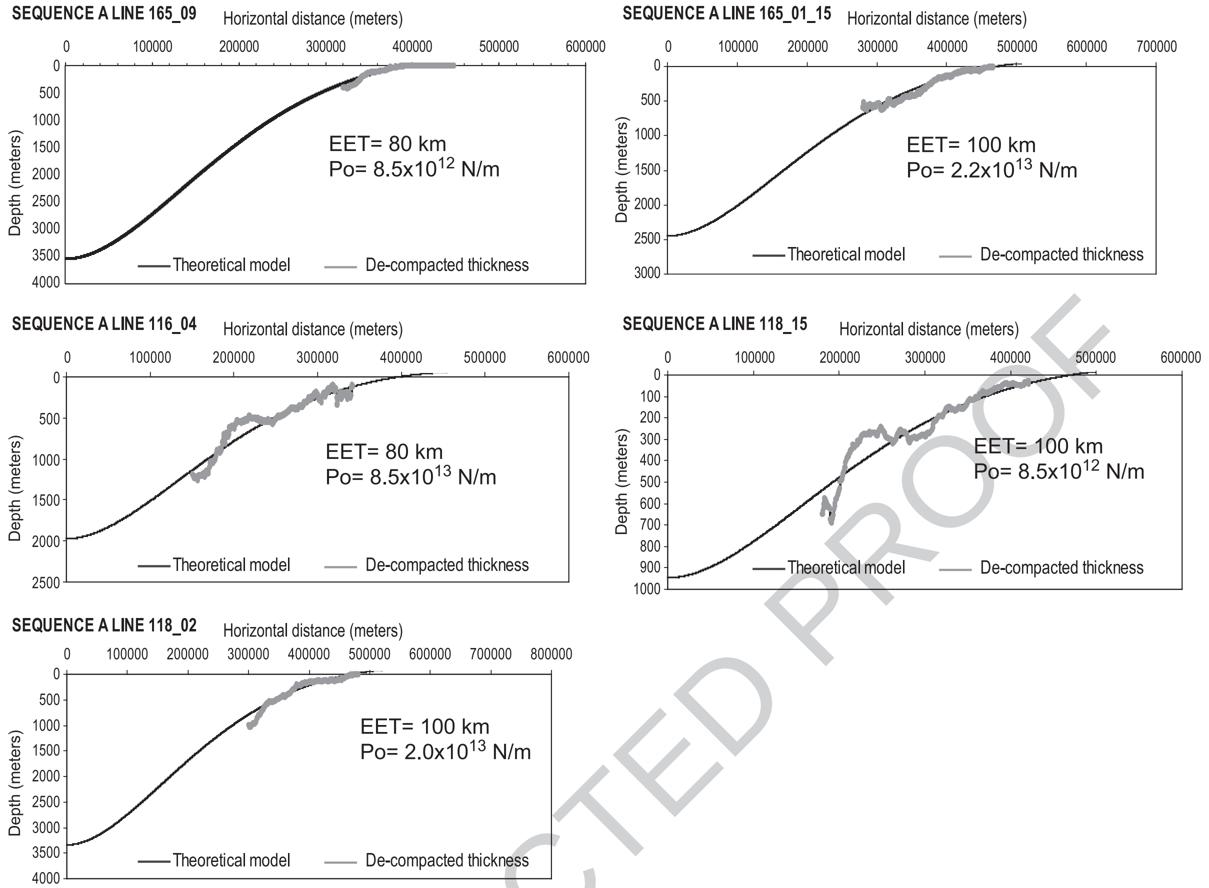

Fig. 5. Flexural model for Sequence A time (~6.5–3.4 Ma). Gray line represents the seismic data (de-compacted thickness). Black line represents the theoretical models. These figures represent the best match between both curves. EET is effective elastic thickness; Po is the amount of load calculated for each model and is located in the most deflected end of the profiles. Note the extent of the deflection between 400 and 470 km.

comparative amount of deformation caused by extension due to flexure. Normal faults caused by plate bending are expected to develop in areas of high curvature. The more flexed the plate is, the higher the curvature, where greater tensional stresses produce brittle deformation (Bradley and Kidd, 1991).

To calculate the apparent displacement in the section along the fault plane in both sequences, vertical stratigraphic separation is measured in meters and corrected by the angle of the fault. The apparent slip separating the reflector representing the top of Sequence A documents not only the displacement of that particular period of deformation, but also subsequent movements. Since we are interested in the apparent slip developed during Sequence A time, it is necessary to subtract any slip up-dip of the fault plane affecting younger deposits. We assume that the fault slip is homogeneous along the entire segment affecting foreland strata. We identify and measure over 200 new or reactivated normal faults active during plate deflection.

5. Results

5.1. Flexure models

Subsidence of the Late Tertiary foreland basin in the Timor Sea is modeled by flexural deformation of a homogeneous, elastic, continuous plate. During

Sequence A time (~6.6–~3,4 Ma) the maximum de-compacted thickness is calculated as ~1200 m along seismic profile 116_04, and the minimum is ~400 m along profile 165_09 (Fig. 5). However, these values are not a direct measure of the deflection of the plate. In order to do that it is necessary to evaluate the position of our data and best fitting models within the regional deflecting trend. A comparison between best fitting curves indicates that during Sequence A time the western part of the Timor Sea was undergoing remarkably more deflection at the end of the effective plate than the eastern part under similar elastic thickness. In contrast, during Sequence B time (~3.4–~1.6 Ma) a com-

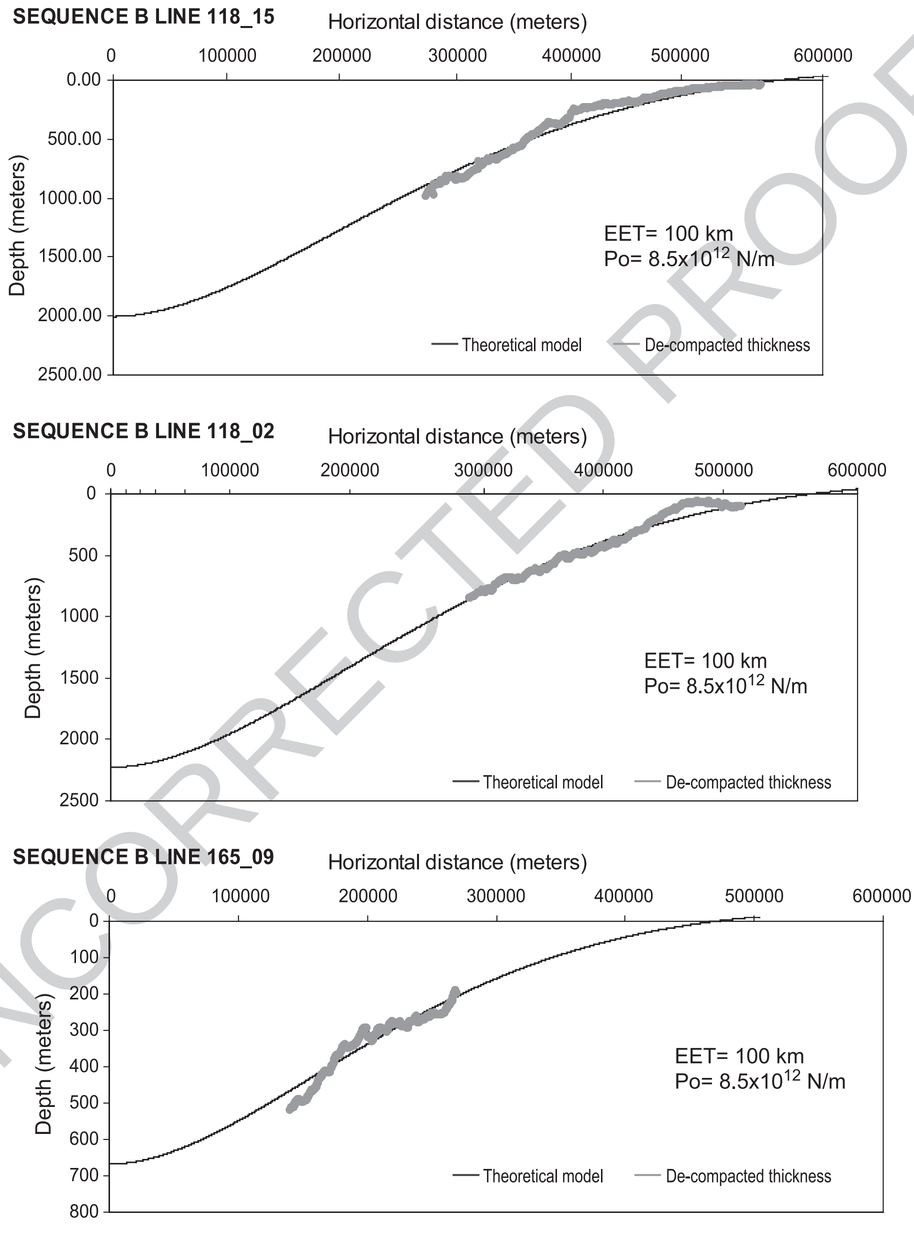

Fig. 6. Flexural models for sequence B. Note the homogeneous effective elastic thickness.

parison of flexural models indicates that the east Timor Sea was undergoing more subsidence (flexure) than the western part. The deposits are thicker in the eastern part of seismic control (up to ~979 m) along lines 118_15 and 118_02 (Fig. 6). During this time the de-compacted thicknesses coincide with predicted values of plate deflection.

A range of effective elastic thickness values (20 to 120 km) is tested, but only cases where values lie between 80 and 100 km appear to match the de-compacted stratigraphic data. For the base of Sequence A in the western-central part of the survey (lines 165_09, 163_01_15, 116_04) effective elastic thickness values between 80 and 100 km produce acceptable fitting curves to the data. In the eastern-most survey area, in turn, only an effective elastic thickness of 100 km appears to fit the seismic data in continuous plate models. Our analysis suggests a maximum deflection of the Australian lithosphere of about 3500 m in the west Timor Sea. Table 2 summarizes the results of the best fitting curves for both sequence times.

5.2. Normal faulting

The tension in the upper-half plate caused by deflection produced abundant normal faulting in the Australian Platform (Figs. 3 and 7). A greater number of faults with higher displacement are found in Late Miocene to Early Pliocene than in Late Pliocene times (Fig. 8a). The distribution of these faults suggests that the stresses caused by vertical loading were probably higher in the west than in the east Timor Sea, as also shown by estimates of curvature (Table 2; Fig. 7). The apparent fault slip measured along the deflected plate shows that the mean displacement during the sequence A period was 40 m in the western area (lines 165_06, 165_09, and 161_03_15) and only ~24 m in the eastern area (lines 118_02, 118_15 and 118_06). Therefore, the average slip is ~66% higher in the west than in the east. The maximum curvature for this period, which occurred toward the west, is $\sim 5.1 \times 10^{-8}$ m. During Sequence B time, normal faulting displacement was also higher in the west Timor Sea. The mean slip is 34 m in this area (lines 165_06, 165_09, and 161_03_15), whereas for the east Timor Sea it is <25 m (lines 118_02, 118_15 and 118_06). The average displacement of these faults is up to 36% higher in the west than in the east (Fig. 8). However, the maximum curvature during this period (~3.4–1.6 Ma) occurs in the east Timor Sea (Table 2) and it is estimated as $\sim 3.2 \times 10^{-8}$ m. Individual fault-slip measurements (Figs. 7 and 8) show that the absolute amount of displacement is up to two times higher in the west Timor Sea (120 m) than in the east Timor Sea (maximum slip of 50 m).

6. Discussion

Variations in the effective elastic thickness of the Australian lithosphere in the Timor Sea are not evident during development of the foreland basin. McNutt (1984) shows that there is a correlation

Table 2
Flexural parameters

Sequence	EET (km)	*D* (Nm)	α (km)	Xo (km)	Po (N/m)	Wo (m)	Xm (km)	*M* (Nm)	*R* (m)
(A)									
165_09	80	4.6e24	168	397	2.7e13	3552	265	2.35e17	5.11e−8
163_01_15	100	9.0e24	199	469	2.2e13	2400	313	2.28e17	2.52e−8
116_04	80	4.6e24	168	397	1.3e13	1940	265	1.31e17	2.84e−8
118_02	100	4.6e24	199	469	2.0e13	2226	313	1.23e17	2.65e−8
118_15	100	9.0e24	199	469	8.5e12	928	313	8.8e16	9.7e−9
(B)									
165_09	100	9.0e24	199	469	1.0e13	655	313	6.21e16	6.87e−9
118_02	100	9.0e24	199	469	2.0e13	2180	313	2.07e17	2.29e−8
118_15	100	9.0e24	199	469	2.8e13	3000	313	2.9e17	3.21e−8

Variables as defined in Table 1. Xo is the distance between the linear load at the position of maximum deflection and the node point or point of zero deflection. Xm is the position of the maximum bending moment along the model.

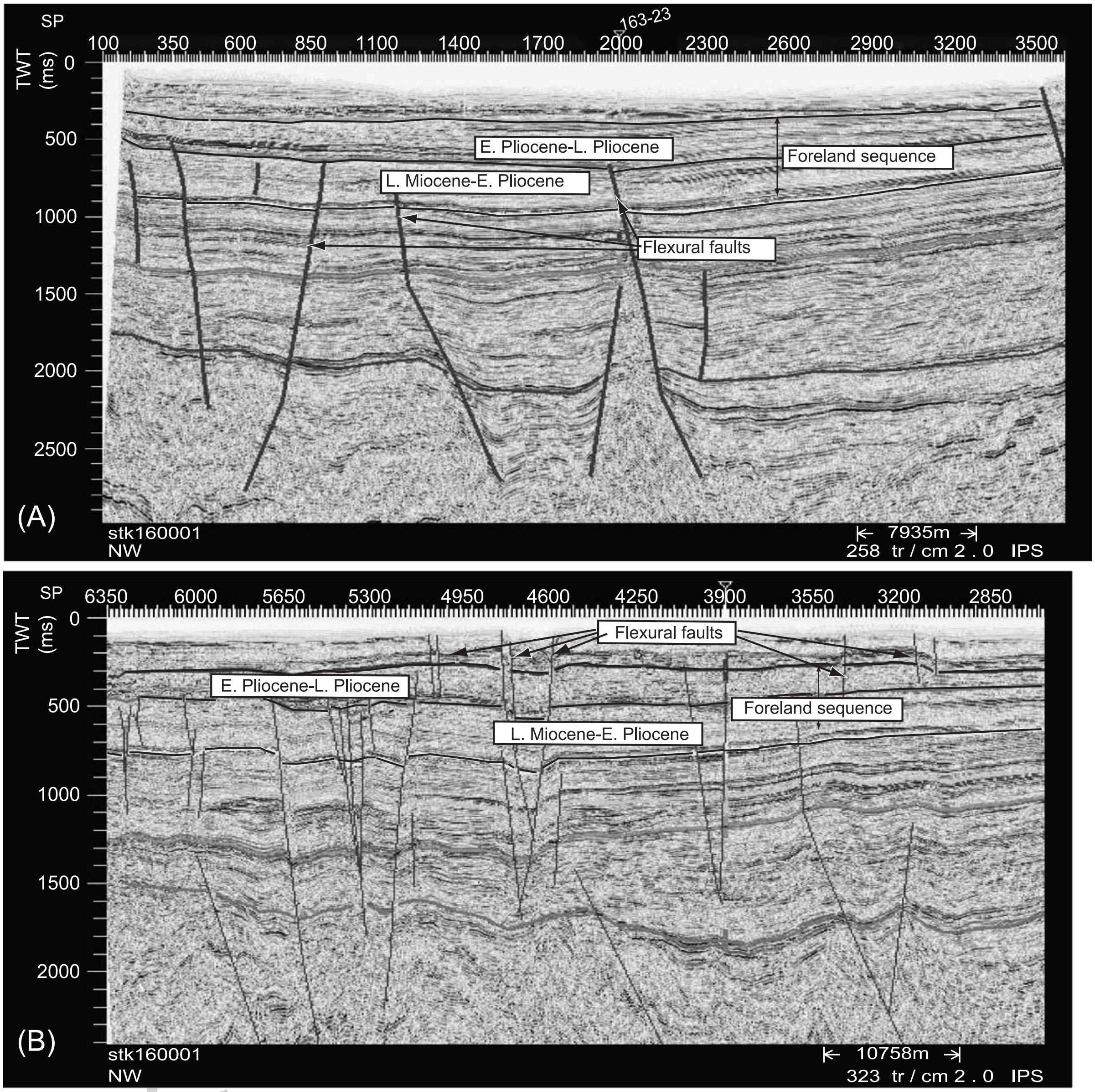

Fig. 7. Normal flexural-related faulting for a section of (A) western line 163_01_15 and (B) eastern line 116_04. Note the Early–Late Pliocene sequence almost unaffected in the western line (A).

between thermal age and plate thickness: plates older than 100 myr are expected to be strong (i.e. high rigidity). By contrast, Watts (2001) notes that no simple relation exists between thermal age and continental lithosphere rigidity. Rather, he favors the role of the crust composition in the present-day geothermal gradient as the key factor controlling the continental effective elastic thickness. Since the last tectonic event to affect the Australian plate prior to bending was Triassic–Jurassic rifting (geothermal age), the Australian continental lithosphere along the northwestern shelf is expected to be strong. At the beginning of continental plate collision, during Sequence A time, models favor an effective elastic thickness ranging

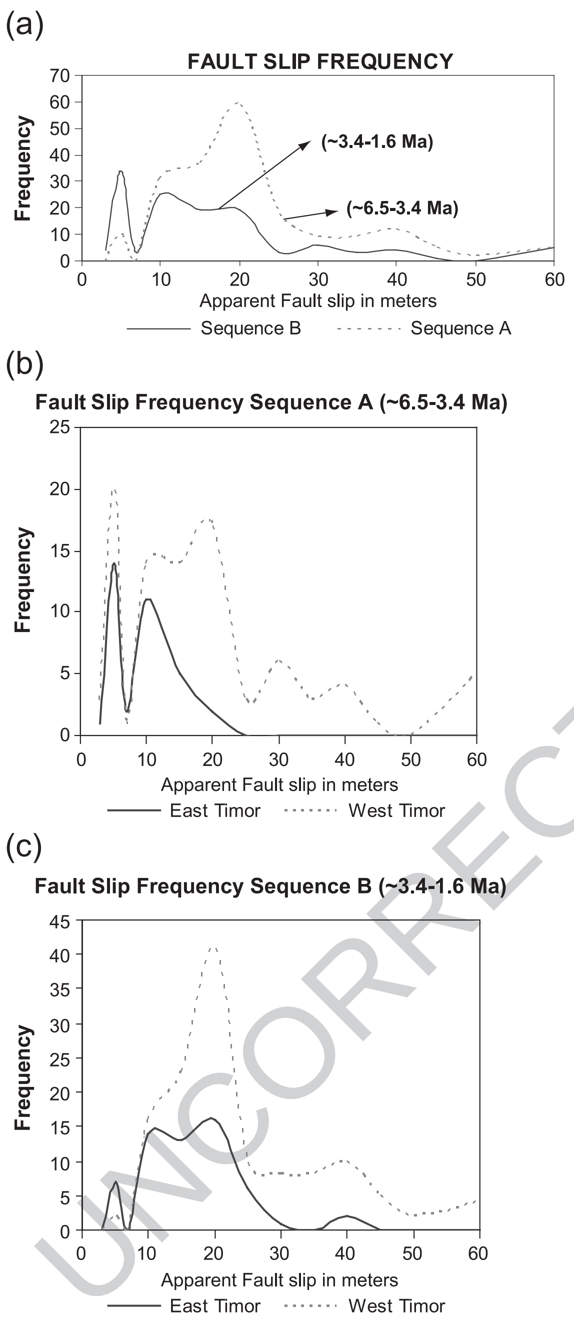

Fig. 8. (a) Fault slip frequency and temporal distribution. Note the higher displacement during Sequence A time than during Sequence B time. In (b) and (c) note the distribution of fault slip along the east and west Timor Sea during foreland evolution.

from 80 to 100 km. The Australian lithosphere in the east Timor Sea appears consistently strong (100 km of effective elastic thickness), while in the central area of the survey (Line 116_04, Figs. 1 and 5) and in the westernmost region of the seismic survey (line 165_09, Figs. 1 and 5) the crust appears weaker, with an effective elastic thickness of 80 km. During Time B, however, all models work with an effective elastic thickness of 100 km (Fig. 6). Noticeably, one best-fitting model, line 165_09, shows changes in effective elastic thickness from 80 to 100 km, from one period to the other, while another, line 118_15, keeps the same elastic thickness of 100 km in both periods. Our range of effective elastic thickness (80 to 100 km) falls within the 25% of uncertainty of estimated accuracy for similar data (Burov and Diament, 1995). These high values probably indicate an unaltered continental lithosphere (no de-coupling) after being tectonically loaded (Burov and Diament, 1995). The relatively constant effective elastic thickness through time rules out any significant weakening of the Australian plate, therefore, no relaxation and/or visco-elastic rheology is necessary to model the basin. Moreover, according to our results, loading appears not to have any weakening effect on the elastic thickness of the Australian plate. This is in agreement with the elastic behavior of the lithosphere during foreland time.

Lateral and spatial variation in crustal strength has been previously reported in foreland basins. For the Bermejo foreland basin in Argentina, Cardozo and Jordan (2001) invoke inherited heterogeneities in pre-bending lithosphere as the cause of these variations. In the Timor Sea, Tandon et al. (2000) develop models of laterally variable effective elastic thickness (25–75 km) due to changes in curvature. Spatial variation in the amount of effective elastic thickness has two probable causes. One could be the effect of an inherited rheologically heterogeneous basement. The central-eastern Timor Sea contains crystalline paleo-highs, which may correspond to regions of higher effective elastic thickness, while the west Timor Sea is affected by ancient basement-grabens filled with pre-Miocene sediments that may decrease lithospheric strength prior to bending (Lavier and Steckler, 1997; Fig. 1). The other probable cause could be lateral variation in strain rate or in strain partitioning, along the collision zone, (Harris, 1991) resulting in differential bending and models of variable lithospheric strength. The foreland sedimentary-cover appears not to have a significant effect in the effective elastic thickness. The Timor Sea foreland sediments do not reach the 3 to 5 km in thickness that according to Lavier and Steckler (1997) are the minimum values necessary to decrease the effective elastic thickness in areas of crust thinner than 35 km.

The change in the modeled deflection through time shows that during Late Miocene–Early Pliocene time the west Timor Sea undergoes greater deflection than the east Timor Sea. The difference at the point of maximum deflection (position of linear load) is about 1000 m (lines 165_09 vs. Line 118_02). However, sediment thickness along the seismic survey shows that foreland sediments in the east are thicker than in the west. This apparent contradiction is resolved if we consider that the two areas represent different lateral positions within a flexural model. The western part of the survey is located farther away from the linear load, and appears thinner in spite of requiring greater deflection. In contrast, the east Timor Sea appears thicker in spite of less flexure at the position of the linear load. During the Late Pliocene, the thickness of the corresponding foreland sequence coincides with the amount of flexure, as the eastern area appears thicker and more deflected than the western part of the survey (Figs. 5 and 6; Table 2). Although in our model the physical causes of loading can be diverse, an end shear vertical force emulates the tectonic (accretionary wedge) and sediment loading. Different shear force values are needed to match the data and are possibly the cause of significant differences in deflection between the eastern and western Timor Sea. It is interesting to note that the amount of deflection (up to ~3500 m) is much larger than the expected subsidence produced by the combination of sea level changes (0–150 m, Haq et al., 1988) and sediment loading. The difference in the modeled deflection between east and west Timor Sea may be due to the polarity of basin closure. Harris (1991) shows an oblique southwestern and northeastern propagation of the collision zone between the Eurasian and Australian plates.

At the end of the Early Pliocene, the theoretical flexure involves ~470 km of Australian plate. The point of maximum deflection and the position of the linear load (Po in Fig. 9) are located northwestward of the present Timor Island (Fig. 9A). The forebulge is between 269 and 310 km wide and ~261 m high. Its top is located in continental Australia, at a point which coincides with today's westernmost Kimberly Highlands (Fig. 9A). By the end of the Late Pliocene (~1.6 Ma), the position of the theoretical point of maximum deflection and linear load (Po) had migrated ~120 km southeastward in the west Timor Sea and ~100 km in the central and east Timor Sea (Fig. 9B). The remaining elements of the flexural model, such as the flexural node (point of zero deflection, Xo in Fig. 9) and the top of the forebulge (Xb in Fig. 9) migrated in the same direction. The displacement of the flexural elements (100 to 120 km) is shorter, although of similar magnitude, than the estimated amount of subducted plate under Eurasia (150 to 200 km). The estimate rates of plate convergence (Tregoning et al., 1994; Genrich et al., 1995) suggest that convergence was not constant during collision. According to our models, at least 570 km of Australian plate have been flexed due to vertical loading. Interestingly, the position of the youngest landward boundary of the regional deflection (Fig. 9B) coincides with the basin-ward boundary of the un-stretched continental crust, in the Kimberly Block area (~35 km), as described in the models of Petkovic et al. (2000). This indicates that only stretched continental crust was flexed during collision in the west Timor Sea.

According to our results, the upper lithosphere was experiencing tension followed by normal faulting coevally with thrusting in the accretionary prism and flexure along the whole Australian shelf. The distribution of normal faulting throughout the entire survey and, according to many authors, along the entire Timor Sea (Baxter et al., 1998; Lorenzo et al., 1998; O'Brien et al., 1996; Woods, 1994), precludes any transmission of large horizontal compressional stresses.

Lorenzo et al. (1998) recognize that the present curvature of the Timor Trough (10^{-7} m^{-1}) appears low compared with values reached by Kruse and Royden (1994) for the Adriatic Sea (10^{-6} m^{-1}). Our models show an even lower maximum curvature value (10^{-8} m^{-1}). According to Watts (2001) and Burov and Diament (1992) curvatures of ~10^{-6} m^{-1} may reduce the effective elastic thickness up to 50%, while values up to 2×10^{-7} m^{-1}

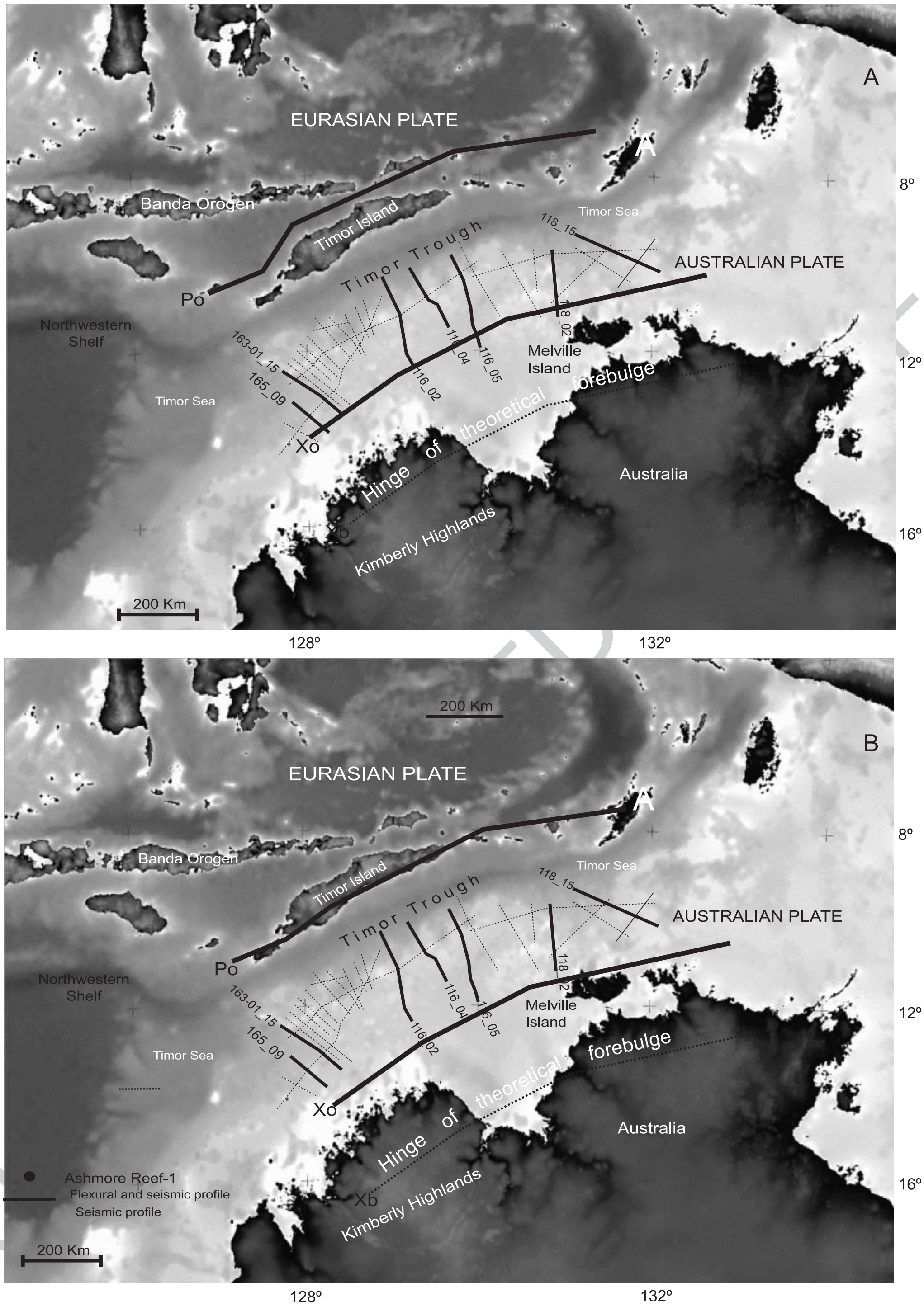

Fig. 9. Late Mioce–Early Pliocene (A) and Late Pliocene (B) geodynamic configuration of Timor Sea. The amount of subducted Australian lithosphere is at least 100 km, according to this model. Effective elastic thickness (EET) is 80 to 100 km for both periods. Flexural variables as defined in Tables 1 and 2. Po: Linear load, Xo: node point (0 deflection), Xb: position of the top of the forebulge.

may reduce the effective elastic thickness up to 20%. Lower values do not represent a significant change in effective elastic thickness. Therefore, according to the values determined in the present study for the periods of time represented by sequences A and B, the curvature should not significantly decrease the effective elastic thickness of the Australian plate during continental collision. This agrees with the invariable effective elastic thickness derived from flexural models.

Low curvature values also agree with the small amount of displacement found in flexure-related normal faults. Although inelastic yielding exists, as established by faulting, it is not enough to change the regional rheology of the plate. Therefore the elastic rheology is consistent with our models. Interestingly, the position of maximum curvature in the west Timor Sea coincides with the position of the Cartier Trough, using 80 and 100 km of elastic thickness for both periods (Figs. 1 and 9). Part of the Cartier Trough deformation may be attributed to high concentration of strain due to flexure.

Kruse and Royden (1994) invoke dynamic stresses, phase changes and conductive heating as causes of reduction in load in the Adriatic Sea through time. However, in the Timor foreland basin the load reduction estimated along the western area is not easily explained using these causes, since it is considered a thermally stable zone. One plausible explanation for the variation in amount of loading in our models is the changing position of the point of maximum bending that migrates towards Australia as the linear load moves in the same direction. The evolution of accretionary prisms conveys continuous development of new faults and related folds, as well as across-the-strike terminations and relays of these structures. These could all be responsible for the adjustment in the amount of loading affecting the plate through time. Harris (1991) shows the change in geometry of the tectonic wedge during the collision of the Australian and Eurasian plates.

According to our models, the vertical shear stress is commensurate in the west and east Timor Sea. However, the amount of deformation due to flexure, implicitly inferred from fault displacement, indicates that the west has supported more cumulative strain than the east. The difference in fault displacement is significant during the Late Miocene–Early Pliocene, as the slip is up to 2.5 times greater in the west than in the east. Increasing deformation in the east Timor Sea during Late Pliocene time probably indicates an increase in the amount of stress propagation in the same direction. This polarity of fault activity in the Australian plate corroborates the oblique nature of plate collision suggested by our models of plate deflection through time and supported by previous works (Harris, 1991; Hamilton, 1979).

7. Summary

During foreland basin evolution (~6.5 to 1.6 Ma.), the effective elastic thickness of the Australian lithosphere in the Timor Sea is between 80 and 100 km. These elastic thickness values agree with the old geothermal age of the Australian Plate. Spatial changes in plate strength are due to heterogeneities prior to bending or basement distribution. The east Timor Sea displays thicker crystalline basement (paleohighs) and appears to be stronger than the west Timor Sea. The latter exhibits thicker pre-bending sedimentary-cover filling wide graben structures. However, the difference in effective elastic thickness between both areas falls within the estimated error.

The effective elastic thickness does not appear to change during foreland basin evolution (~6.5. to 1.6 Ma). Consequently, no visco-elastic relaxation can be inferred from the flexure of the plate during loading. Foreland sediment cover is too thin to cause any lithospheric weakening. Curvature of the Australian plate in the Timor Sea is low when compared to other foreland basins. The small curvature was not enough to weaken the lithosphere in the area. Accordingly, normal faulting exhibits small apparent slip (up to 150 m). Moreover, inelastic yielding appears not to affect the regional rheology of the Australian lithosphere.

According to our models, at least 570 km of the Australian plate (mostly areas of stretched continental crust) was flexed due to vertical loading during the collision. However, the deflection at one particular time involved only 400 to 470 km (most of the Australian Platform). As the tectonic loading advanced towards continental Australia (100 to 110 km), an increasing portion of the Australian plate became flexed. These figures correspond to the estimated value of subducted plate. According to our models, the point of maximum deflection was located under today's accretionary prism during the entire period of foreland evolution. The top of the forebulge was located in continental Australia, and is partially represented by the Kimberly Highlands.

The deflection of the plate caused by tectonic loading was at a maximum in the west Timor Sea (up to 3500 m) at the beginning of the collision and at a maximum in the east Timor Sea (up to 2300 m) by the end of the convergence. This eastward propagation of the deflection indicates the oblique polarity of the collision between the Eurasian and Australian plates.

Flexure-related normal faulting corroborates the oblique character of the collision. Faulting begins to affect the plate in the west Timor Sea at the beginning of convergence and propagates eastward in the same direction as deflection. The west Timor Sea exhibits higher accumulated deformation due to a longer time of loading and coeval bending of the plate.

Acknowledgements

We thank Dr. Geoff O'Brian and the Australian Geological Survey Organisation (AGSO) for allowing us to use the seismic data. We also express gratitude to Unavco-GMT for permission to use their programs and data for preparing part of the maps. We are grateful to Dr. Patricia Londono for her help with the preparation of this manuscript.

References

Allen, H., Allen, J., 1990. Basin Analysis. Blackwell, Oxford, UK, pp. 262–281.

Apthorpe, M., 1988. Caionozoic depositional history of the North West Shelf. In: Purcell, P., Purcell, R. (Eds.), The North West Shelf of Australia. Petroleum Exploration Society of Australia, Perth, Australia, pp. 55–84.

Audley-Charles, M., 1986. Timor–Tanimbar trough: the foreland basin of the evolving Banda orogen. In: Allen, P.A., Homewood, P. (Eds.), Foreland Basin. Blackwell, Oxford, UK, pp. 91–102.

Baxter, K., Hill, K., Cooper, T., 1998. Quantitative modeling of the Jurassic–Holocene subsidence history of the Vulcan Sub-basin, North West Shelf: constraints on lithosphere evolution during continental breakup. Australian Journal of Earth Sciences 45, 143–154.

Beamont, C., 1981. Foreland basins. Geophysics Journal Research of Astronomical Society 65, 471–498.

Boheme, R., 1996. Stratigraphic response to Neogene tectonism on the Australian Northwestern Shelf. Masters Thesis, Louisiana State University, Baton Rouge, USA.

Bradley, D., Kidd, W., 1991. Flexural extension of the upper continental crust in collisional foredeeps. Geological Society of America Bulletin 103, 1416–1438.

Burov, E., Diament, M., 1992. Flexure of the continental lithosphere with multilayered rheology. Geophysical Journal 109, 449–468.

Burov, E., Diament, M., 1995. The effective elastic thickness (Te) of continental lithosphere: what does it really mean? Journal of Geophysical Research 100, 3905–3927.

Cardozo, N., Jordan, T., 2001. Causes of spatially variable tectonic subsidence in the Miocene Bermejo foreland basin. Argentina Basin Research 13, 335–358.

Dorobek, S., 1995. Synorogenic carbonate platforms and reefs in foreland basin: controls in stratigraphic evolution and platform/reef morphology. In: Dorobek, S., Ross, G. (Eds.), Stratigraphic Evolution of Foreland Basins. SEPM Spec. Publ., vol. 52, pp. 127–148.

Genrich, J., Bock, Y., McCaffrey, R., Calais, E., Stevens, C., Rais, J., Subarya, C., Puntodewo, S., 1995. Kinematics of the eastern Indonesia Island Arc estimated by global positioning system measurements. EOS, Trans. AGU 75, 162.

Hamilton, W., 1979. Tectonics of the Indonesian Region. US Govt. Printing office, Washington, USA.

Haq, B., Handerbol, J., Vail, P., 1988. Mesozoic and Cenozoic chronostratigraphic and eustatic cycles. In: Wilgus, C., Hasting, B., Kendal, C., Posamentier, H., Ross, Ch., Wagoner, V. (Eds.), Sea Level Changes: An Integrated Approach. SEPM Spec. Publ., vol. 42, pp. 71–108.

Harris, R., 1991. Temporal distribution of strain in the active Banda orogen: a reconciliation of rival hypothesis. Journal of Southeast Asian Science 6, 371–386.

Hillis, R., 1990. Post-Permian subsidence and tectonics, Vulcan sub-basin, North West Shelf, Australia. Pacific Rim Congress. Australian Institute of Mining and Metallurgy, Victoria, Australia, pp. 203–211.

Hillis, R., 1992. Evidence of Pliocene erosion at Ashmore reef (Timor Sea) from the sonic velocities of Neogene Limestone formations. Exploration Geophysics 23, 489–495.

Karig, D., Barber, A., Charltan, T., Klemperer, S., Hussong, D., 1987. Nature and distribution of deformation across the Banda Arc–Australian Collision zone at Timor. Geological Society of America Bulletin 98, 18–32.

Kruse, S., Royden, L., 1994. Bending and unbending of an elastic lithosphere: the Cenozoic history of the Apennine and Dinaride foredeep basins. Tectonics 13, 278–302.

Lavier, L., Steckler, M., 1997. The effect of sedimentary cover on the flexural strength of continental lithosphere. Nature 389, 476–479.

Lerche, I., 1990. Philosophies and strategies of model building. In: Cross, T. (Ed.), Quantitative Dynamic Stratigraphy, pp. 21–44.

Lorenzo, J., O'Brien, G., Stewart, J., Tandon, K., 1998. Inelastic yielding and forebulge shape across a modern foreland basin:

North west shelf of Australia, Timor Sea. Geophysical Research Letters 25, 1455–1458.

McNutt, M., 1984. Lithospheric flexure and thermal anomalies. Journal of Geophysical Research 89, 11180–11194.

Miall, A., 1995. Collision-related foreland basins. In: Busby, C., Ingersoll, R. (Eds.), Tectonics of Sedimentary Basin. Blackwell, Oxford, UK, pp. 393–424.

O'Brian, G., Lisk, M., Duddy, I., Hamilton, J., Woods, J., Cowley, R., 1999. Plate convergence, foreland development and fault reactivation: primary control on brine migration, thermal histories and trap breach in the Timor Sea, Australia. Marine and Petroleum Geology 16, 533–560.

O'Brien, G., Etheridge, M., Willcox, J., Morse, M., Symonds, P., Norman, C., Needham, D., 1993. The structural architecture of the Timor Sea, North western Australia: implications for basin development and hydrocarbon exploration. APPEA Journal 34, 258–278.

O'Brien, G., Higgins, R., Symonds, P., Quaife, P., Colwell, J., Blevin, J., 1996. Basement control on the development of extensional systems in Australia's Timor Sea: an example of hybrid hard linked/soft linked faulting? APPEA Journal 36, 161–200.

Ostby, J., Johnstone, C., 1994. The role of regional seismic surveys in the exploration of the North West Shelf. In: Purcell, P., Purcell, R. (Eds.), The Sedimentary Basins of Western Australia. Proceedings of the West Australian Basin Symposium, Perth, Australia, pp. 211–222.

Petkovic, P., Collins, C., Finlayson, D., 2000. A crustal transect between Precambrian Australia and the Timor Trough across the Vulcan Sub-basin. Tectonophysics 329, 23–38.

Richardson, A., Blundell, D., 1996. Continental collision in the Banda arc. In: Hall, R., Blundell, D. (Eds.), Tectonic Evolution of South East Asia. Geological Society of London Special Publication, vol. 106, pp. 47–60.

Steckler, M., Watts, A., 1980. The Gulf of Lion: subsidence of a young continental lithosphere. Nature 287, 135–139.

Tandon, K., Lorenzo, L., O'Brien, G., 2000. Effective elastic thickness of the northern Australian continental lithosphere subducting beneath the Banda Orogen (Indonesia): inelastic failure at the start of continental subduction. Tectonophysics 329, 39–60.

Tregoning, P., Brunner, F., Bock, Y., Puntodewo, S., McCaffrey, R., Genrich, J., Calais, E., Rias, J., Subarya, C., 1994. First geodetic measurement of convergence across the Java Trench. Geophysics Research Letters 21, 2135–2138.

Turcotte, D., Schubert, G., 1982. Geodynamics. Application of Continuum Physics to Geological Problems. Wiley, New York, USA.

Veevers, J., 1974. Sedimentary sequences of the Timor Trough, Timor, and the Sahul Shelf. In: Veevers, J., Heirtzler, J., et al., (Eds.), Initial Reports of the Deep Sea Drilling Project, vol. 27, pp. 567–569.

Watts, A., 2001. Isostasy and Flexure of the Lithosphere. Cambridge Univ. Press, Cambridge UK.

Woods, E., 1994. A salt related detachment model of the development of the Vulcan sub-basin. In: Purcell, P., Purcell, R. (Eds.), The Sedimentary Basins of Western Australia. Proceedings of the West Australian Basin Symposium, Perth, Australia, pp. 259–274.

Wormald, G., 1988. The geology of the Challis–Oilfield–Timor Sea, Australia. In: Purcell, P., Purcell, R. (Eds.), The North West Shelf of Australia. Petroleum Exploration Society of Australia, Perth, Australia, pp. 425–438.

Yang, K., Dorobek, S., 1995. The Permian basin of west Texas and New Mexico: tectonic history of a composite foreland basin and its effects on stratigraphic development. In: Dorobek, S.L., Ross, G.M. (Eds.), Stratigraphic Evolution of Foreland Basins. SEPM Spec. Publ., vol. 52, pp. 149–174.